Available online at www.sciencedirect.com
SCIENCE DIRECT®
Polymer 44 (2003) 4355–4362
polymer
www.elsevier.com/locate/polymer

Spherulitic morphology and crystallization kinetics of melt-miscible blends of poly(3-hydroxybutyrate) with low molecular weight poly(ethylene oxide)

Jiang-Wen You[a], Hsiu-Jung Chiu[a,*], Trong-Ming Don[b]

[a]*Department of Chemical Engineering, Ta Hwa Institute of Technology, Chiunglin, Hsinchu 30703, Taiwan, ROC*
[b]*Department of Chemical Engineering, Tamkang University, Tamsui, Taipei County 25147, Taiwan, ROC*

Received 14 June 2002; received in revised form 27 December 2002; accepted 5 April 2003

Abstract

The spherulitic morphology and crystallization kinetics of the blends of poly(3-hydroxybutyrate) (PHB) with the low molecular weight poly(ethylene oxide) (PEO) prepared by the solution casting have been investigated by differential scanning calorimetry and polarized optical microscopy. The blend was a crystalline/amorphous system when temperatures lie between the melting point of PEO (T_m^{PEO} = ca. 60 °C) and that of PHB (T_m^{PHB} = ca. 170 °C), while it became a crystalline/crystalline system below T_m^{PEO}. With PHB crystallization at the crystallization temperature (T_c) of 70 °C, the blends showed PHB banded spherulitic texture, which could be perturbed by the subsequent PEO crystallization in PEO-rich compositions upon further cooling to room temperature. When PHB and PEO were allowed to crystallize upon quench from melt to room temperature, fairly competitive crystallization emerged where crystallization and segregation of PHB and PEO may occur simultaneously, leading to a complicated spherulitic morphology. As for the results of crystallization kinetics, the PHB crystallization exothermic temperature (T_f^{PHB}) on cooling, PHB spherulitic growth rate (G_{PHB}), and overall crystallization rate of PHB (k_n) exhibited maxima in their dependences of PEO composition. This was attributed to the coupling between enhanced chain mobility and depression in equilibrium melting point (T_m^0), since the low molecular weight PEO has a very low glass transition temperature (T_g) over the T_c range studied, G_{PHB} increased with T_c but k_n was found to decrease. The drop of k_n with increasing T_c was therefore predominately governed by the large depression in nucleation rate at higher T_c.

Keywords: Spherulitic morphology; Crystallization kinetics; Poly(3-hydroxybutyrate)

1. Introduction

The crystallization kinetics of the melt-miscible blends of crystalline and amorphous polymers has been extensively studied [1–15]. When crystallization occurs below the melting point of the crystalline component, the process involves two types of polymer transport, namely, diffusion of the crystallizable component toward the crystal growth front and a simultaneous rejection of the amorphous component. This crystallization process produces a liquid–solid phase separation, leading to a variety of morphological patterns closely governed by the kinetics of the two types of polymer transport. In this case, the morphological formation may be kinetically controlled by the thermal history and composition to achieve tailor-made properties for the blends. Therefore, investigation of the crystallization kinetics of polymer blends containing crystallizable components also has the practical significance.

The morphology induced by liquid–solid phase separation in crystalline/amorphous blends has also been studied extensively. The morphological patterns are characterized by the distance of the segregation of the amorphous diluent, where three basic types can be defined: (1) interlamellar segregation, where segregation of the amorphous component occurs at the lamellar level, so that the amorphous component is located in interlamellar regions; (2) interfibrillar segregation, where the amorphous component is segregated by a larger distance to the regions between the lamellar bundles in spherulites; (3) interspherulitic segregation, where the amorphous region is segregated by the largest distance to the regions between spherulites [16–18].

* Corresponding author.

0032-3861/03/$ - see front matter © 2003 Elsevier Science Ltd. All rights reserved.
doi:10.1016/S0032-3861(03)00348-3

A blend system does not necessarily display only one type of morphology. Different types of morphologies may coexist, leading to the multiple locations for the amorphous component.

Bacterially synthesized poly(3-hydroxybutyrate) (PHB) is a crystalline polymer with biodegradability and biocompatibility, which are attractive for application in the present environment [19–21]. PHB has some disadvantages such as high brittleness, poor processability, and poor thermal stability. The high brittleness was thought to arise from the large spherulitic nature associated with the crystallization of PHB. Since the spherulite size is determined by the competition between nucleation and growth rates, the disadvantages due to spherulite size the properties could be circumvented by controlling PHB crystallization kinetics. Blending could be an efficient approach for such purpose, because PHB crystallization is affected due to the presence of a second component.

Crystallization kinetics in melt-miscible blends of crystalliine/amorphous polymers with PHB, such as PHB/poly(epichlorohydrin) (PECH) [1,2], PHB/poly(vinyl acetate) (PVAc) [3–5], and PHB/atactic-PHB [6,7], PHB/poly(vinyl phenol) (PVPh) [8,9], has been extensively studied. These systems showed depression of crystallization kinetics of PHB with the addition of amorphous component. The melt-miscible crystalline/crystalline blends with PHB, such as PHB/poly(vinylidene fluoride) (PVDF) [22–24] and PHB/poly(ethylene oxide) (PEO) [25–28], were less studied. The morphology of crystalline/crystalline blends is expected to be more complex than that of crystalline/amorphous systems due to the interplay between two crystallization processes. For PHB/PVDF blends, owing to the proximity of melting points, PHB and PVDF crystallized over essentially the same temperature range and consequently created a crystalline/crystalline state with a morphology characterized by the spatial arrangement of PHB and PVDF lamellae [24]. Marand et al. [22,23] have found that the PVDF α-crystal spherulites always formed prior to PHB, and PHB spherulites must progress past existing PVDF spherulites because it was developed after an induction period that was long enough to allow for the PVDF spherulites to grow to their full extent. Therefore, it is difficult to investigate PHB crystallization kinetics in the crystalline/amorphous state in PHB/PVDF blends, where the crystallization of PVDF always occurs easily prior to PHB. However, in the PHB/PEO blends, the crystalline/amorphous and crystalline/crystalline states can be distinguished due to the large melting point difference between PHB and PEO. Martuscelli et al. [25] found that when PHB/PEO blends were located in the crystalline/amorphous state, the PHB spherulitic growth rate (G_{PHB}) decreased with increasing PEO content, which was similar to that found in other crystalline/amorphous PHB blends. Martuscelli et al. [25] also reported that the PEO crystal or the lamellar domain existed within PHB spherulites in the crystalline/crystalline state, and this was attributed to the segregation of amorphous PEO into the interlamellar or interfibrillar regions of PHB during PHB crystallization above T_m^{PEO}.

In the present study, we are also interested in the PHB/PEO blends because PEO is a hydrophilic thermoplastic commodity polymer having excellent miscibility with PHB. In contrast to the previous study [25], the PEO with low molecular weight ($M_w = 5000$) and lower T_g (ca. −80 °C) is used to blend with PHB. In this case, it will be shown that the rate of PHB can actually be promoted by blending with PEO, in contrast to the previous results. The spherulitic morphologies in the crystalline/amorphous and crystalline/crystalline states of the PHB/low-M_w PEO blends and the variation of the crystallization kinetics with composition and crystallization temperature will be discussed in detail.

2. Experimental

2.1. Materials and samples preparation

PHB with $M_n = 2.93 \times 10^5$ and $M_w = 6.5 \times 10^5$ and PEO with $M_w = 5000$ were purchased from Aldrich Chemical Co. PHB was blended with PEO by solution casting. The blending components were dissolved in DMF at room temperature yielding a 1 wt% solution. The solution was subsequently poured onto a Petri dish and the blend film was obtained after evaporating most of the solvent on a hot plate at ca. 90 °C. The blend film was further dried in a vacuum oven at 50 °C for at least 24 h till constant sample weight. TGA measurement of the dried films showed negligible weight loss above the boiling point of DMF, indicating nearly complete removal of solvent for the blend films.

2.2. Polarized optical microscopy

The spherulitic morphology and growth rate were monitored with a Pac Hund polarized optical microscope. The sample was first melt on a Linkam HFS901 hot stage at 190 °C for 1 min, then quickly transferred to another hot stage equilibrated at the desired crystallization temperature (T_c), where spherulitic growth was monitored. Micrographs were taken at intervals for measuring the spherulite radii (R) at various time periods. The growth rate was calculated from the change of spherulitic radius with time, dR/dt.

2.3. Differential scanning calorimetry

The calorimetry experiments were carried out using TA Instrument 2000 differential scanning calorimetry (DSC). For the glass transition temperature (T_g) experiment, the sample was first heated at a heating rate of 20 °C/min from room temperature to 190 °C, maintained at 190 °C for 1 min, and then was rapidly quenched to −160 °C with liquid N_2 to minimize the crystallinity in the sample.

Subsequently, the samples were heated a second time at the same heating rate to obtain (T_g). The crystallization exothermic peak temperature (T_f) was measured while the blend was cooled non-isothermally from the melt at a cooling rate of 5 °C/min. For the isothermal crystallization experiment, each sample was first melted on a Linkam HFS901 hot stage at 190 °C for 1 min, and then rapidly transferred into DSC equilibrated the desired (T_c) to allow crystallization. The isothermal crystallization exotherm was recorded. The resultant exotherm was used to obtain the relative degree of crystallinity, $X(t)$, viz.

$$X(t) = \frac{\int_0^t \left(\frac{dH}{dt}\right)dt}{\int_0^\infty \left(\frac{dH}{dt}\right)dt} \quad (1)$$

where the numerator represents the area of isotherms accumulated as of time t and the denominator is the total exotherm area.

3. Results and discussion

3.1. Miscibility

Fig. 1 shows the composition dependence of (T_g). The (T_g) of neat PHB and PEO were 2.6 °C and −79.2 °C, respectively. Each blend displayed only one composition-dependent (T_g), meaning that the blends were miscible in the melt. The (T_g)-composition relation can be described well by the Fox equation [29]:

$$\frac{1}{T_{g(blend)}} = \frac{W_{PHB}}{T_{g(PHB)}} + \frac{W_{PEO}}{T_{g(PEO)}} \quad (2)$$

where $T_{g(blend)}$, $T_{g(PHB)}$ and $T_{g(PEO)}$ are T_gs of blend, PHB, and PEO, respectively, while w_{PHB} and w_{PEO} stand for the weight fractions of PHB and PEO. This T_g-composition dependence was also consistent with that found in the literature [25–28], which indicated that PHB and PEO have achieved molecular level of mixing.

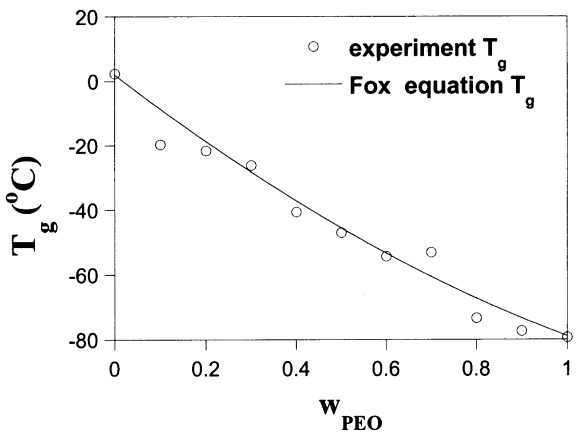

Fig. 1. T_g-composition dependence of PHB/PEO blends.

3.2. Spherulitic morphology

PHB and PEO are both crystalline polymers with melting points of ca. 170 and 60 °C, respectively. At temperatures between 60 and 170 °C, the blend is a crystalline/amorphous system but it becomes as crystalline/crystalline system below 60 °C. Fig. 2 shows the banded PHB spherulites of neat PHB and PHB/PEO blends crystallized at 70 °C (a crystalline/amorphous state). For all the compositions studied, PHB spherulitic growths were observed to be linear with time and no apparent evidence of liquid–liquid phase separation was found up to the point of spherulite impingement. This implies that PEO was contained within the PHB spherulites during PHB crystallization at 70 °C. The spherulitic band spacing increased with increasing PEO content. Barham [19] found that the band spacing was broader at higher T_c for neat PHB. Therefore, the effect of the addition of PEO on the band spacing is equivalent to increase in T_c. A similar conclusion was also drawn for the PVDF/poly(butylene adipate) (PBA) blends [30] where the band spacing of PVDF spherulites increased with increasing T_c or PBA content.

After the morphology of the crystalline/amorphous state shown in Fig. 2 was formed, the samples were directly transferred to another hot stage at room temperature to allow the subsequent crystallization of PEO, while then yielded the morphology of the crystalline/crystalline state. The texture of the original PHB banded spherulites was not influenced by the later PEO crystallization for the composition range from PHB/PEO 100/0 to 50/50. It may be suggested that the tiny crystals of PEO could grow in the PHB interfibrillar regions for those PHB-rich compositions. However, for PEO-rich compositions (i.e. 40/60 to 10/90 blends), we observed the growth of PEO crystals across the

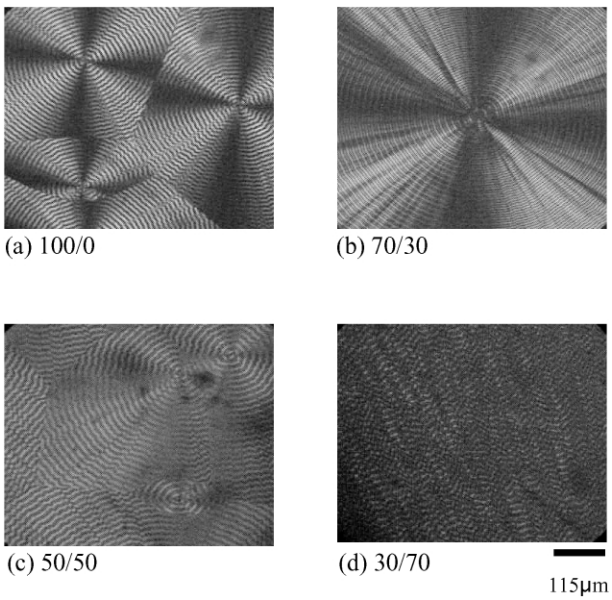

Fig. 2. Banded spherulitic structures of PHB in PHB/PEO blends crystallized at T_c = 70 °C (a) 100/0, (b) 70/30, (c) 50/50, (d) 30/70.

existing PHB spherulites and consequently disturbed the texture of PHB spherulites. For example, in 20/80 blend as shown in Fig. 3, the later PEO crystal growth disturbed the original banded feature of PHB spherulites drastically, showing that the subsequent crystallization of PEO at room temperature occurred in the spatially confined interfibrillar regions within the PHB spherulites.

The crystallizations of PHB and PEO were quite competitive when the blends were directly quenched from melt to room temperature. The spherulitic morphology of crystalline/crystalline blends, crystallized by direct quench to room temperature are shown in Fig. 4. In contrast to that in the crystalline/amorphous state, the spherulitic textures exhibited quite complex patterns and were strongly influenced by blend compositions. The spherulites of neat PEO displayed a smooth and clear Maltese-cross pattern as shown in Fig. 4(a), but the PEO-rich composition of 20/80 showed a coarse PEO spherulitic texture with a disruption of Maltese-cross pattern as shown in Fig. 4(b). In the PEO-rich compositions, PEO crystallization proceeded prior to PHB crystallization upon quenched to room temperature. Disruption of Maltese-cross pattern basically indicates the intraspherulitic segregation of PHB during the crystallization of PEO. On the other hand, for PHB-rich compositions where PHB crystallization occurred prior to PEO crystallization, the resultant spherulitic morphology was characterized by the dominant PHB banded spherulitic texture, as shown in Fig. 4(c), indicating the intraspherulitic segregation of PEO during the crystallization of PHB. These observations reveal that the spherulitic morphology of the crystalline/crystalline PHB/PEO generated by direct crystallization at room temperature is largely affected by the blend composition where the major component always dominates the spherulitic formation. This is by contrast to that found in other crystalline/crystalline blends such as PVDF/PBA [30], and PVDF/poly(butylene succinate) [31], where the higher-T_m PVDF component always crystallized prior to the lower-T_m component. The difference observed here might be due to the low molecular weight of PEO used.

As the temperature was raised to 70 °C, the PEO crystals in Fig. 4 were melted to create a crystalline/amorphous state as shown in Fig. 5. It was found that the original PEO spherulitic texture of 20/80 blend in Fig. 4(b) has

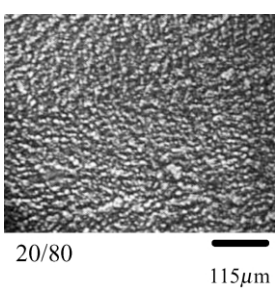

Fig. 3. Optical micrograph showing the variation in the spherulitic morphology of 20/80 composition under room temperature (After PHB first crystallized at T_c = 70 °C, then PEO crystallized at room temperature).

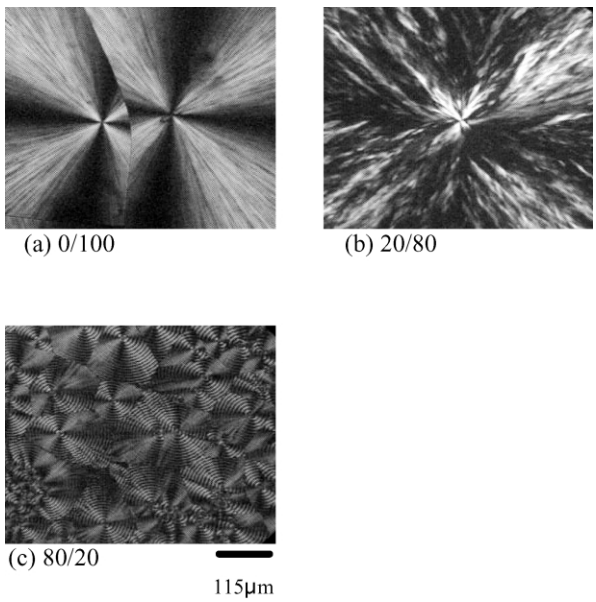

Fig. 4. Spherulitic morphology of PHB/PEO blends crystallized by direct quench to room temperature (PHB and PEO simultaneously crystallized at room temperature)(a) 0/100, (b) 20/80, (c) 80/20.

transformed into the strip feature, as shown in Fig. 5(a). The fragmentary PHB crystal masked within the PEO spherulite caused the strip fibril. It may be suggested that while PEO crystallization has occurred prior to PHB at room temperature, the temporarily amorphous PHB was segregated into the interfibrillar regions of PEO and subsequently crystallized. PHB crystals not only existed in PEO interfibrillar regions but were also covered by the PEO crystals under polarized optical microscopy (POM). In the case of PHB-rich blends, we found that the original PHB spherulitic texture in Fig. 4(b) was not influenced at all on heating to 70 °C, as demonstrated in Fig. 5(b). This may imply that PEO was probably unable to crystallize or just formed tiny crystals totally masked by the PHB crystals at room temperature in these PHB-rich compositions.

3.3. Crystallization exothermic temperature

As PHB/PEO blends were cooled non-isothermally from

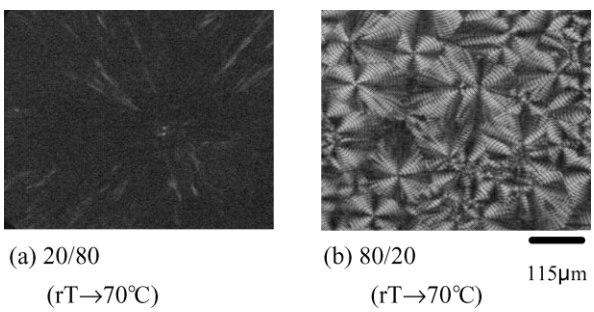

Fig. 5. Optical micrograph showing the variation in the spherulitic morphology melted PEO crystals under 70 °C (After PHB and PEO have first crystallized at room temperature, then PEO crystals were melted by the temperature raised to 70 °C) (a) 20/80, (b) 80/20.

the melt at a given cooling rate of 5 °C/min in DSC, the corresponding thermograms showed two distinct crystallization exothermic peaks. Clearly, the peak at the higher temperature reflects the heat emitted during the crystallization of PHB (denoted at T_f^{PHB}), and the other peak at the lower temperature is attributed to PEO crystallization (denoted at T_f^{PEO}). Fig. 6 shows the dependence of T_f^{PHB} and T_f^{PEO} on w_{PEO} at the cooling rate of 5 °C/min. Because, T_f^{PHB} was higher than T_f^{PEO} at each blend composition, the crystallization of PHB always occurred prior to that of PEO; therefore PHB and PEO crystallizations can be easily separated under such a non-isothermal cooling. It can be seen that the T_f^{PHB} of neat PHB was about 63 °C and slightly increased with increasing w_{PEO} up to $w_{PEO} = 0.2$. It is reasonable to assume that the molecular mobility of PHB was enhanced due to the addition of lower T_g PEO, which thereby promoted the crystallization kinetics of PHB. On the other hand, addition of PEO caused large depression in T_m^0, which would lead to reduction in PHB crystallization rate. Consequently, the combination of enhanced molecular mobility and T_m^0 depression resulted in the maximum of T_f^{PHB} at $w_{PEO} = 0.2$. The crystallization of PEO was also affected by the presence of PHB. T_f^{PEO} of neat PEO was about 35 °C, and it reached a maximum at $w_{PEO} = 0.9$. Since PHB crystallized prior to PEO during the cooling process, the existing PHB crystals could offer surface nucleation site for PEO, which promoted PEO crystallization rate at 10/90 composition. Further increase in PHB content caused depression in T_m^0 to dominate, and hence resulted in decrease of crystallization rate. It should be noted that the composition dependence of T_f^{PHB} and T_f^{PEO} observed here were not in agreement with those reported previously [25,26] showing monotonic decreases of both T_f^{PHB} and T_f^{PEO} instead of a maximum. The difference may be attributed to the different molecular weight of PEO used. The molecular weight of PEO used here was 5000 (compared with $M_{PEO} = 20,000$ in the previous studies); the PEO with lower molecular weight served as a more effective promoter for PHB molecular mobility and consequently enhanced the PHB crystallization rate at low to moderate PEO composition.

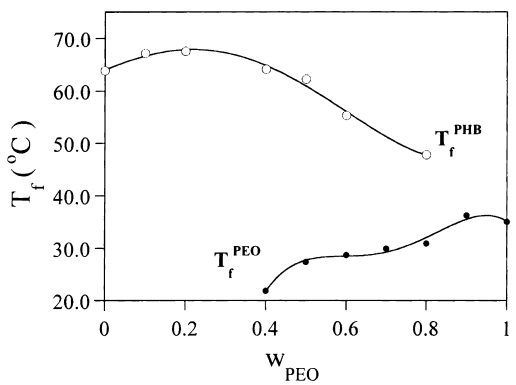

Fig. 6. Variations of T_f^{PHB} and T_f^{PEO} with the composition of w_{PEO} at a cooling rate of 5 °C/min.

3.4. Spherulitic growth rate

Fig. 7 depicts the variation of PHB spherulitic growth rate (G_{PHB}) with w_{PEO} at various T_cs. Similar to T_f^{PHB}, G_{PHB} curves in Fig. 7 show maxima for all the T_cs investigated. Again, the interplay between enhanced molecular mobility and depression in T_m^0 caused the composition dependence of G_{PHB} to show a maximum near $w_{PEO} = 0.5$. This observation is different from that reported by Martuselli et al. [25], where G_{PHB} was found to depress monotonously with increasing w_{PEO}. The difference was attributed to the lower PEO molecular weight used and different T_c range explored in this study. It is well known that the crystallization window of a crystalline polymer must lie between T_g and T_m^0. When the desired T_cs locate toward T_g, the crystallization kinetics would be controlled by the chain mobility, such that the rate increases with increasing T_c in this mobility regime. In contrast, if the desired T_cs are located toward T_m^0, the crystallization rate would be governed by the thermodynamic driving force of crystallization (the thermodynamically controlled regime). The interplay between these two factors produces a maximum in crystallization rate at T_c^{max} between T_g and T_m^0. T_c^{max} of neat PHB or PHB in blends was reported to be in the neighborhood of 90 °C [6,32,33]. In this study, since the investigated T_cs were located below 90 °C, G_{PHB} was governed by the mobility and hence G_{PHB} increased with increasing T_c for each composition. However, in the study reported by Martuselli et al. [25], T_cs explored were higher than 90 °C, so that the G_{PHB} decreased with increasing T_c due to thermodynamically controlled behavior. Therefore, it may be suggested that if the desired T_cs lie in the mobility-controlled regime, the dependence of G_{PHB} on w_{PEO} would show a maximum due to the combined effect of enhanced molecular mobility and depression in T_m^0. Conversely, when the desired T_cs lie in the thermodynamically controlled regime, G_{PHB} was predominately influenced by the depression in T_m^0, and thus composition dependence of G_{PHB} did not exhibit a maximum.

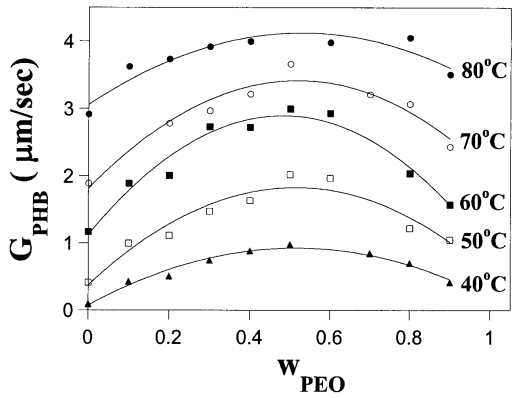

Fig. 7. PHB spherulitic radial growth rate (G_{PHB}) with the composition of w_{PEO}.

The spherulitic growth kinetics of blends containing one crystallizable polymer has been described by Eq. (3) [34,35].

$$A = \log G_{PHB} - \log \Phi_2 + \frac{U^*}{2.3R(T_c - T_\infty)} - \frac{0.2T_m^0 \ln \Phi_2}{2.3\Delta T} = \log G_o - \frac{K_g}{2.3T_c\Delta T f} \quad (3)$$

where G_o is a pre-exponential factor that is weakly of temperature. ΔT is the degree of supercooling ($\Delta T = T_m^0 - T_c$), Φ_2 is the volume fraction of PHB, which can be obtained using the densities of amorphous PHB and PEO (i.e. $\rho_{PHB} = 1.17$ g/cm^3 [19], $\rho_{PEO} = 1.08$ g/cm^3 [36]), $U^*/2.3R(T_c - T_\infty)$ is the contribution arising from the diffusion of crystallizable (PHB) and diluent (PEO) involved in the crystallization, the quantity U^* is the sum of activation energies of chain motion of PHB and PEO in the melt. T_∞ is the temperature below which such motions cease ($T_\infty = T_g - C$; C = constant). f is a correction factor that accounts for the dependence of the heat of fusion on temperature and is written as $f = 2T_c/(T_m^0 + T_c)$. The parameter K_g is the nucleation factor expressed as:

$$K_g = \frac{\alpha b_o \sigma \sigma_e T_m^0}{\Delta H^0 k} \quad (4)$$

where b_o is the thickness of a monomolecular layer, s and s^e are the lateral and end surface free energies, respectively. ΔH^0 is the heat of fusion of completely crystalline PHB and k is the Boltzmann constant. According to the Hoffman–Laurentzen theory [37,38], the value of α depends on the regime of crystallization. When T_cs lie in regime I (lower ΔT) or regime III (high ΔT) $\alpha = 4$, while $\alpha = 2$ for regime II growth process (medium ΔT).

The left-hand term (A) of Eq. (3) was plotted against $1/2.3T_c\Delta Tf$, with all T_m^0 values obtained from the results reported by Martuselli et al. [25]. C was chosen as $51.6K$ and U*(1500 ~ 2200cal/mol) was varied to maximize the correlation coefficient of the linear line. The results are shown in Fig. 8. The values of K_g calculated from the slope are listed in Table 1. It is seen that K_g of neat PHB was twice as large as that of blends. Barham et al. [19] also found $\alpha = 4$ for neat PHB and regime III was assigned. The crystallization of PHB in the blends was considered to occur in regime II, corresponding to $\alpha = 2$. These results are similar to those previously obtained by Martuscelli et al. [25] and other blends with PHB such as PHB/PECH [1], PHB/PVAc [3] and PHB/a-PHB [6].

Table 1
K_g and growth regime of PHB/PEO blends

PHB/PEO	K_g	Regime
100/0	4.0120×10^5	III
90/10	2.1191×10^5	II
80/20	1.4389×10^5	II
70/30	2.3766×10^5	II
60/40	2.0133×10^5	II
50/50	2.5353×10^5	II

Fig. 9 depicts the spherulitic growth rate of PEO (G_{PEO}) at $T_c = 25$ and 40 °C as a function of w_{PEO}. It is observed that G_{PEO} increased with increasing w_{PEO} at a given T_c and decreased with increasing T_c, signifying that the driving force of crystallization dominates the crystal growth kinetics. Comparing with G_{PHB}, G_{PEO} was found to be much larger than G_{PHB} at the same crystallization temperature.

3.5. Overall crystallization kinetic

Fig. 10 shows the temporal development of overall crystallinity of PHB, $X(t)$, for various compositions at $T_c =$ 60 °C. It can be seen that the crystallization isotherms displayed the characteristic sigmoidal shape. The half-time of crystallization, $t_{0.5}$, defined as the time required to attain half of the final crystallinity, was evaluated from these curves. The overall crystallization rate can be represented by $1/t_{0.5}$. Fig. 11 displays the variation of $1/t_{0.5}$ with w_{PEO} at various T_cs. The curves also displayed maximum near

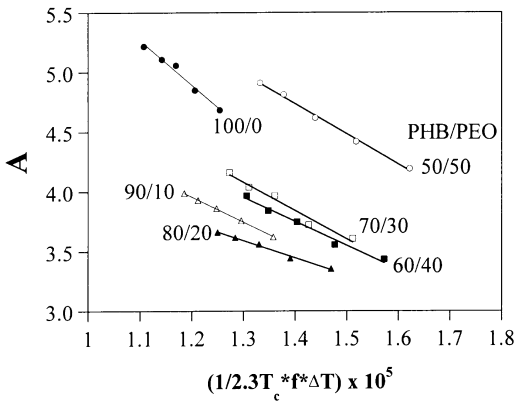

Fig. 8. Plot of the left-hand side of Eq. (3) vs $1/(2.3T_c\Delta Tf)$ for PHB/PEO blends.

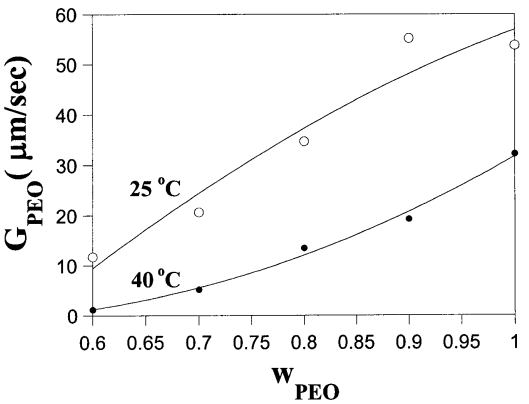

Fig. 9. PEO spherulitic radial growth rate (G_{PEO}) with the composition of w_{PEO} at $T_c = 25$ and 40 °C.

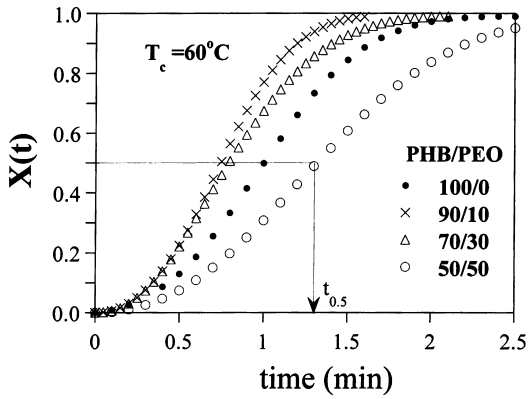

Fig. 10. Crystallization isotherm of PHB/PEO blends at $T_c = 60$ °C.

$w_{PEO} \cong 0.1$. Again, this is attributed to the combined effects of enhanced chain mobility and depression in T_m^0 of PHB as previously stated for G_{PHB} (Fig. 7). It was noticed that the composition where the maxima were located toward $w_{PEO} \cong 0.1$ and the height of the maximum decreased with increasing T_c. This means that the effect of enhanced molecular mobility diminished with increasing T_c. In addition, the tendency that $1/t_{0.5}$ decreases with increasing T_c is opposite to that of G_{PHB}, meaning that the overall crystallization kinetics was mainly dominated by the nucleation rate. This correlation would be further judged through the determination of the overall crystallization rate constant (k) by the Avrami equation [39–41] viz.

$$\ln\{-\ln[1-X(t)]\} = \ln k + n \ln t \quad (5)$$

where k is the overall crystallization rate constant containing contributions from both nucleation and growth rates. n is the Avrami exponent which depends on the nucleation and growth mechanism. The plot of $\ln\{-\ln[1-X(t)]\}$ vs $\ln t$ produces a linear line with the intercept and slope given by k and n, respectively. Fig. 12 displays the Avrami plot of neat PHB at $T_c = 60$ °C. It can be seen that the experimental data closely agree with the Avrami equation at low conversion. The plot at high conversion deviates from the equation due to the occurrence of secondary crystallization [42,43].

The rate constant defined in Eq. (5) has the unit of min^{-n}.

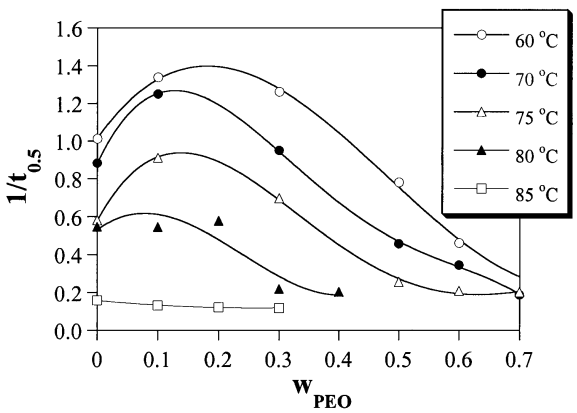

Fig. 11. Variation of $1/t_{0.5}$ with the composition of w_{PEO} at various T_cs.

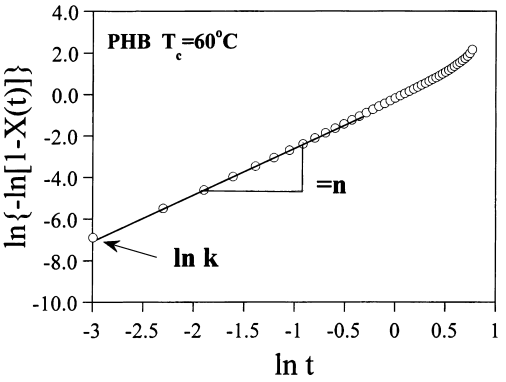

Fig. 12. Plot of the Avrami equation analysis of neat PHB at $T_c = 60$ °C.

In this study, we modified the rate constant as $k_n = k^{1/n}$ to unify the unit of the rate constant as min^{-1}. Fig. 13 depicts the variation of k_n with w_{PEO} at various T_cs. The composition dependence on k_n closely follows that of $1/t_{0.5}$ (Fig. 11), namely, both $1/t_{0.5}$ and k_n showed the maxima, and the height of the maxima decreased with increasing T_c. This provides further evidence that the overall crystallization rate was controlled by the nucleation rate.

The values of n were about 2.5 ± 0.3 and almost independent of composition and crystallization temperature, which is typically observed among crystalline blends [1,44,45]. Such values of n were thought to be due to the existence of mixed growth, surface nucleation, and two-step crystallization. Grenier et al. [45] have also ascribed the observed n to experimental factors, such as an erroneous determination of the 'zero' time. However, though all n values were less than three, they may roughly confirm a three-dimensional (spherulitic) growth process initiated by heterogeneous nucleation, which is consistent with the observed spherulitic morphology by POM. The results also indicate that the nucleation mechanism and growth geometry of PHB crystals were unaffected by the addition of PEO.

According to three-dimensional spherulitic growth, k is defined as:

$$k = 4\pi N_\rho (G_{PHB})^3/3 \quad (6)$$

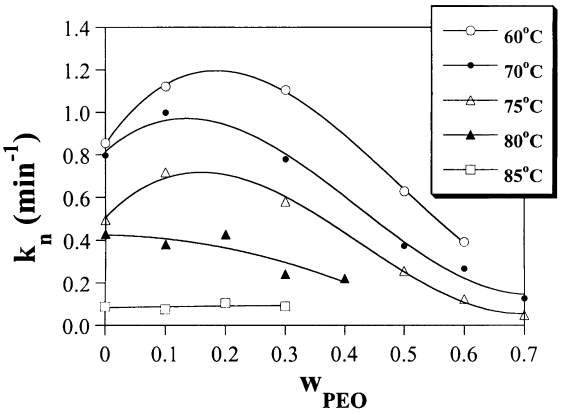

Fig. 13. Variation of k_n with the composition of w_{PEO} at various T_cs.

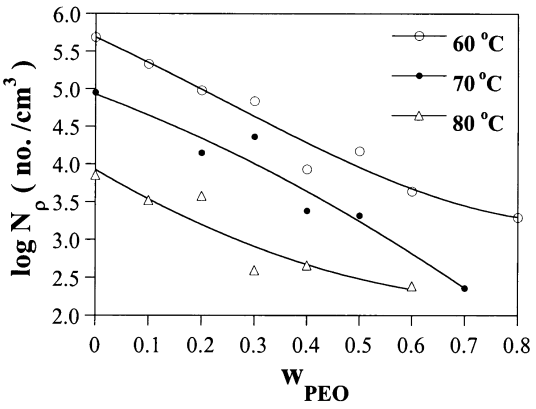

Fig. 14. Variation of log N_ρ with the composition of w_{PEO} at various T_cs.

where N_ρ is the nucleation density corresponding to the number of nuclei per cm^3. From Eq. (6) the values of N_ρ are calculated. Fig. 14 depicts the variation of log N_ρ with w_{PEO}. It can be seen that log N_ρ dramatically decreased with increasing w_{PEO} at a given T_c or with increasing T_c at a given blend composition. This indicates that the addition of PEO suppressed the PHB nucleation rate, but promoted the growth rate. This result confirms that the overall crystallization rate was mainly controlled by nucleation rate.

4. Conclusion

The blends of PHB with low molecular weight PEO were miscible in the melt. Crystallization of PHB at $T_c = 70$ °C generated banded PHB spherulitic texture, which could be disturbed by the subsequent PEO crystallization in PEO-rich compositions. Direct cooling from melt to room temperature produced a rather competitive crystallization between PHB and PEO, where the crystallization and segregation of both PHB and PEO occurred competitively, leading to quite complicated spherulitic morphology. While the PHB/PEO blends were cooled non-isothermally from the melt at a rate of 5 °C/min, the DSC thermograms showed two distinct crystallization exothermic temperatures of PHB and PEO (T_f^{PHB} and T_f^{PEO}). Because, T_f^{PHB} was higher than T_f^{PEO} at each blend composition, PHB and PEO crystallization can be easily separated under such a non-isothermal cooling process. Composition variation of T_f^{PHB}, G_{PHB}, $1/t_{0.5}$ and k_n displayed maxima, attributable to combined effects of enhanced molecular mobility and depression of T_m^0. PHB nucleation density (N_ρ) dramatically decreased with increasing PEO content. From the crystal growth kinetics analysis, neat PHB was found to exhibit regime III growth while the blends showed regime II growth process under the supercooling studied.

Acknowledgements

This work was supported by the National Science Council, ROC, under Grant NSC 91-2216-E-233-001.

References

[1] Paglia ED, Beltrame PL, Canetti M, Seves A, Marcandalli B, Martuscelli E. Polymer 1993;34:996.
[2] Sadocco P, Canetti M, Seves A, Martuscelli E. Polymer 1993;34:3368.
[3] Greco P, Martuscelli E. Polymer 1989;30:1475.
[4] An Y, Dong L, Xing P, Mo Z, Zhuang Y, Feng Z. Eur Polym J 1997;33:1449.
[5] Chiu HJ, Chen HL, Lin TL, Lin JS. Macromolecules 1999;32:4969.
[6] Peace R, Brown GR, Marchessault RH. Polymer 1994;35:3984.
[7] Abe H, Doi Y, Satkowski MM, Noda I. Macromolecules 1994;27:50.
[8] Iriondo P, Iruin JJ, Fernandez-Berrodi MJ. Polymer 1995;36:3235.
[9] Xing P, Dong L, An Y, Feng Z, Avella M, Martuscelli E. Macromolecules 1997;30:2726.
[10] Chitrangad B, Middleman S. Macromolecules 1981;14:352.
[11] Liu AS, Liar WB, Chiu WY. Macromolecules 1998;31:6593.
[12] Martuscelli E, Silverstre C, Gismondi C. Makromol Chem 1985;186:16.
[13] Alfonso GC, Russell TP. Macromolecules 1986;19:1143.
[14] Greveceur G, Groeninckx G. Macromolecules 1991;24:1190.
[15] Cheung YW, Stein RS. Macromolecules 1994;27:2512.
[16] Stein RS, Khambatta FB, Warner FP, Russell T, Escala A, Balizer E. J Polym Sci: Polym Symp 1978;63:313.
[17] Russell TP, Ito H, Wignall GD. Macromolecules 1988;21:1703.
[18] Defleuw G, Groeninckx G, Renaers H. Polymer 1989;30:595.
[19] Barham PJ, Keller A, Otun EL, Holmes P. J Mater Sci 1984;19:2781.
[20] Griffin GJL. Chemistry and technology of biodegradable polymers p.48.
[21] Erhoogt H, Ramsay BA, Favis BD. Polymer 1994;35:5155.
[22] Marand H, Collins M. ACS Polym Prepr 1990;31:552.
[23] Edie SL, Marand H. ACS Polym Prepr 1991;32:329.
[24] Chiu HJ, Chen HL, Lin JS. Polymer 2001;42:5749.
[25] Avella M, Martuscelli E. Polymer 1988;29:1731.
[26] Avella M, Martuscelli E, Greco P. Polymer 1991;32:1647.
[27] Avella M, Martuscelli E, Raimo M. Polymer 1993;34:3234.
[28] Kumagai Y, Doi Y. Polym Degrad Stab 1992;35:87.
[29] Fox TG. Bull Am Phys Soc 1956;2:1123.
[30] Penning JP, Manley R st. J. Macromolecules 1996;29:84.
[31] Lee JC, Tazawa H, Ikehara T, Nish T. Polym J 1998;30:327.
[32] Abe H, Matsubara I, Doi Y. Macromolecules 1995;28:844.
[33] Lotti N, Pizzoli M, Ceccorulli G, Scandola M. Polymer 1993;34:4935.
[34] Hoffman JD. Polymer 1982;24:3.
[35] Boon J, Azcue JM. J Polym Sci: Polym Phys 1968;6:885.
[36] Talibuddin S, Wu L, Runt J. Macromolecules 1996;29:7527.
[37] Lauritzen JI, Hoffman JD. J Appl Phys 1973;44:4340.
[38] Mandelkern L, Quinm FA, Flory PJ. J Appl Phys 1954;25:830.
[39] Avrami MJ. Chem Phys 1939;7:1103.
[40] Avrami MJ. Chem Phys 1940;8:212.
[41] Avrami MJ. Chem Phys 1941;9:177.
[42] Hillier IH. J Polym Sci, A 1965;3:3067.
[43] Price PP. J Polym Sci, A 1965;3:3079.
[44] Hay JN, Sharma L. Polymer 2000;41:5799.
[45] Grenier D, Prud'hamme R. J Polym Sci: Polym Phys 1980;18:1655.